Cell Calcium 78 (2019) 26–34

Contents lists available at ScienceDirect

Cell Calcium

journal homepage: www.elsevier.com/locate/ceca

Discovery and characterization of a positive allosteric modulator of transient receptor potential canonical 6 (TRPC6) channels

S. Häfner, N. Urban, M. Schaefer*

Rudolf-Boehm-Institute of Pharmacology and Toxicology, Medical Faculty, Leipzig University, Härtelstraße 16-18, 04107 Leipzig, Germany

ARTICLE INFO

Keywords:
Transient receptor potential channel
Compound library screening
Calcium ion influx
Patch clamp electrophysiology
Positive allosteric modulator
Platelets

ABSTRACT

The non-selective second messenger-gated cation channel TRPC6 (transient receptor potential canonical 6) is activated by diacylglycerols (DAG) in a PKC-independent manner and plays important roles in a variety of physiological processes and diseases. In order to facilitate novel therapies, the development of potent inhibitors as well as channel-activating agents is of great interest. The screening of a chemical library, comprising about 17,000 small molecule compounds, revealed an agent, which induced increases in intracellular Ca^{2+} concentrations ($[Ca^{2+}]_i$) in a concentration-dependent manner (EC_{50} = 2.37 ± 0.25 μM) in stably TRPC6-expressing HEK293 cells. This new compound (**C20**) selectively acts on TRPC6, unlike OAG (1-oleoyl-1-acetyl-*sn*-glycerol), which also activates PKC and does not discriminate between TRPC6 and the closely related channels TRPC3 and TRPC7. Further evaluation by Ca^{2+} assays and electrophysiological studies revealed that **C20** rather operated as an enhancer of channel activation than as an activator by itself and led to the assumption that the compound **C20** is an allosteric modulator of TRPC6, enabling low basal concentrations of DAG to induce activation of the ion channel. Furthermore, **C20** was tested in human platelets that express TRPC6. A combined activation of TRPC6 with **C20** and OAG elicited a robust increase in $[Ca^{2+}]_i$ in human platelets. This potentiated channel activation was sensitive to TRPC6 channel blockers. To achieve sufficient amounts of **C20** for biological studies, we applied a one-pot synthesis strategy. With regard to studies in native systems, the sensitizing ability of **C20** can be a valuable pharmacological tool to selectively exaggerate TRPC6-dependent signals.

1. Introduction

Within the large superfamily of transient receptor potential (TRP) channels, the canonical TRPC channels were first identified in *Drosophila melanogaster*, and later on found to form a family of seven Ca^{2+}-permeable, non-selective cation channels (TRPC1-7) in mammals [1,2]. Among them, TRPC1, 4 and 5 form a closely related subgroup as well as TRPC3, 6 and 7. The sequences of the TRPC3/6/7 subgroup display a close relationship with up to 78% amino acid identity. The physiological activation of these channels is mediated by DAGs, produced by hydrolysis of phosphatidylinositol 4,5-bisphosphate (PIP_2) in consequence of GPCR stimulation or PLC activation [3]. TRPC6 is abundantly expressed in various tissues and, amongst others, described in pulmonary and vascular smooth muscle cells [4], brain [5] and kidney [6] as well as in immune cells and platelets [7,8]. Connected to these reports are several descriptions of pathologies, which are associated with dysfunctions or mutations in the TRPC6 gene, like focal segmental glomerulosclerosis or pulmonary hypertension [9–11]. In the last decade, several modulators of TRPC6 have been described, beginning from poorly potent inhibitors like SKF96365 [12] and 8009-5364 [13] with IC_{50} values in the lower micromolar range leading to recent blockers like SAR7334 [14] and SH045 [15], which display nanomolar affinities and a TRPC6-specific subtype selectivity. The development of TRPC6 activators has also advanced. However, agonists like GSK1702934 A [16], piperazine derivatives [17] and the just recently reported pyrazolopyrimidines [18] still lack subtype selectivity within the TRPC3/6/7 group of ion channels. With the intention to find a more TRPC6-selective agonist, we performed a medium throughput screening of a chemical library, which resulted in the identification of a small molecule TRPC6 modulator, displaying selectivity versus TRPC3 and TRPC7. Here, we describe its re-synthesis and characterization in heterologous cell models as well as in natively TRPC6-expressing cells.

Abbreviations: BIM-1, bisindolylmaleimide 1; *DAG*, diacylglycerol; *DAGK*, diacylglycerol kinase; *FCS*, fetal calf serum; *FLIPR*, fluorescence imaging plate reader; *OAG*, 1-oleoyl-1-acetyl-*sn*-glycerol; *PAM*, positive allosteric modulator; *PKC*, protein kinase C; *PLC*, phospholipase C; *PIP2*, phosphatidylinositol 45-bisphosphate; *PMA*, phorbol 12-myristate 13-acetate; *PRP*, platelet rich plasma; *ROCE*, receptor-operated calcium entry; *TRPC*, transient receptor potential canonical

* Corresponding author.
E-mail address: michael.schaefer@medizin.uni-leipzig.de (M. Schaefer).

https://doi.org/10.1016/j.ceca.2018.12.009
Received 5 October 2018; Received in revised form 20 December 2018; Accepted 20 December 2018
Available online 21 December 2018
0143-4160/

2. Methods

2.1. Synthesis of 3-(6,7-dimethoxy-3,3-dimethyl-3,4-dihydroisoquinolin-1-yl)-2H-chromen-2-one (compound C20)

3-Cyanocoumarin (408 mg, 2.38 mmol, 1.0 eq.) was mixed with isobutyraldehyde (172 mg, 2.38 mmol, 1.0 eq.) and 1,2-dimethoxybenzene (330 mg, 2.38 mmol, 1.0 eq.). While stirring the mixture, concentrated sulphuric acid (5 mL) was added dropwise over a time of 15 min at 0 °C. The reaction was stirred for 30 min at 0 °C before addition of 50 mL ice cold water. The reaction mixture was extracted five times with toluene. The pH of the aqueous phase was adjusted to 8–9 with ammonium carbonate. The slightly yellow precipitate was filtered off, washed with ice cold water and dried (184 mg, 0.51 mmol, 21%). **^{1}H-NMR** (400 MHz, $CDCl_3$) δ [ppm] = 7.99 (s, 1 H), 7.61-7.53 (m, 2 H), 7.41-7.28 (m, 2 H), 6.70 (s, 1 H), 6.66 (s, 1 H), 3.92 (s, 3 H), 3.75 (s, 3 H), 2.78 (s, 2 H), 1.30 (s, 6 H). **^{13}C-NMR** (101 MHz, $CDCl_3$) δ [ppm] = 160.0, 159.8, 154.4, 151.7, 147.4, 143.5, 132.1, 130.2, 128.5, 128.0, 124.6, 119.9, 119.2, 116.7, 111.3, 110.1, 56.4, 56.0, 54.9, 38.3, 27.6, 27.5. **HRMS (ESI)** *m/z*: calc. for $C_{22}H_{22}NO_4$ $(M+H)^+$: 364.1549; found: 364.1544. $\mathbf{R_f}$ (*n*-pentane/Et_2O = 3/2): 0.31. $[\alpha]_{589}^{20}$ ($CHCl_3$, c = 1.0): +57.0°. **UV-vis** (H_2O): λ_{max} / nm (ε / M^{-1} cm^{-1}) = 279 (sh), 318 (23,200), 377 (sh). More detailed analytical methods and data are provided in the Supplementary Information.

2.2. Cell culture

Parental human embryonic kidney (HEK) 293 cells were grown in Earle's Minimum Essential Medium (MEM) supplemented with 10% fetal calf serum (FCS), 2 mM *l*-glutamine, 100 units/mL penicillin and 0.1 mg/mL streptomycin. Stably transfected cell lines ($HEK_{hTRPC3\text{-}YFP}$, $HEK_{mTRPC4\beta\text{-}YFP}$, $HEK_{mTRPC5\text{-}YFP}$, $HEK_{hTRPC6\text{-}YFP}$, $HEK_{hTRPC7\text{-}YFP}$, $HEK_{hTRPA1\text{-}YFP}$, $HEK_{rTRPV1\text{-}CFP}$, $HEK_{rTRPV2\text{-}YFP}$, $HEK_{rTRPV3\text{-}YFP}$, HEK_{hTRPM2}, $HEK_{mTRPM3\text{-}YFP}$, $HEK_{hTRPM8\text{-}CFP}$) were generated and maintained as described previously [13,19]. All cells were grown at 37 °C in a humidified atmosphere containing 5% CO_2.

2.3. Fluorometric [Ca^{2+}] measurements

Fluorometric [Ca^{2+}] measurements were performed as described previously [19,20]. The assays were performed in HEPES-buffered saline (HBS), containing 132 mM NaCl, 6 mM KCl, 1 mM $MgCl_2$, 1 mM $CaCl_2$, 5.5 mM D-glucose and 10 mM HEPES adjusted to pH 7.4 with NaOH. The buffer was supplemented with 0.1% bovine serum albumin (BSA) and 0.02% pluronic F127. For single-cell $[Ca^{2+}]_i$ experiments, stably TRPC6-transfected or parental HEK293 cells were seeded on poly-L-lysine-coated 24 mm glass coverslips 24 h before the experiment. Cells were loaded in HBS containing 0.2% BSA for 30 min at 37 °C with 2 μM fura-2/AM. The coverslips were mounted in a bath chamber and superfused. The $[Ca^{2+}]_i$ measurements were performed on an inverted epifluorescence microscope with a Fluar 10 × /0.5 objective (Carl Zeiss, Jena, Germany), and calibrated as described [19,21]. For fluorescence imaging plate reader (FLIPR) measurements, cells were harvested and loaded with 4 μM fluo-4/AM in culture medium for 30 min at 37 °C. Measurements were carried out in a custom-made fluorescence imaging plate reader built into a robotic liquid handling station (Freedom Evo 150, Tecan, Männedorf, Switzerland). Fluo-4 was excited at 450–470 nm by means of an LED array, and emitted light was imaged through a 515 nm long pass filter with a scientific CMOS camera (Zyla 5.5, Andor Technology Ltd., Belfast, UK). Compounds were added with a 96-tip multichannel arm (MCA96, Tecan) at the indicated final concentrations during the recording and incubated for 2 min before cells were stimulated with agonist. During injections, fluorescence images were continuously monitored under control of the Micromanager software [22]. Fluorescence intensities in single wells were calculated with ImageJ software [23], corrected for the respective background signals and normalized to the initial intensities (F/F_0).

2.4. PKCε translocation studies

Stably transfected $HEK_{PKCe\text{-}YFP}$ cells [24] were plated on coverslips 24 h prior to the experiment. The translocation of PKC to the membrane was monitored on an inverted LSM 510 META confocal microscope (Carl Zeiss), using a Plan-Apochromat 100x/1.46 objective (Carl Zeiss) and applying pinhole settings to yield optical slices with a thickness of 0.6–0.8 μM. Excitation wavelength was 514 nm and emission was filtered with a 530 nm long-pass filter. Cells were challenged with 15 μM **C20**, followed by 50 μM OAG and 1 μM phorbol 12-myristate 13-acetate (PMA) in intervals of 60 s, each.

2.5. Electrophysiology

For the electrophysiological EC_{50} determination, $HEK_{hTRPC6\text{-}YFP}$ cells were seeded at low density on poly-L-lysine-coated glass coverslips 24 h before the experiment. Whole cell currents were recorded at room temperature, using a Multiclamp 700B amplifier with a Digidata 1440 A digitizer (Axon CNS, Molecular Devices) controlled by the PClamp 10 software (Molecular Devices). During the experiment, cells were superfused with standard extracellular solution (140 mM NaCl, 5 mM CsCl, 2 mM $MgCl_2$, 1 mM $CaCl_2$, and 10 mM HEPES, 0.1% BSA, pH 7.4 adjusted with NaOH). The intracellular solution contained 140 mM CsCl, 4 mM $MgCl_2$, 10 mM EGTA, and 10 mM HEPES adjusted to pH 7.2 with CsOH. Patch pipettes were prepared with a PIP6 pipette puller (HEKA) from borosilicate glass capillaries (Science Products) and had a resistance of 4–10 MΩ when filled with intracellular solution. For current/voltage (I/V) analysis, voltage ramps from -100 mV to + 100 mV at a speed of 500 mV/ms were applied in 1-s intervals. Currents were filtered at 3 kHz with a four-pole Bessel filter and sampled at 10 kHz. The series resistance was compensated by 70%.

2.6. Isolation of human platelets

Blood was obtained from healthy volunteers who had abstained from any medicals for at least 7 days. The blood (16–32 mL) was drawn from the cubital vein with a 21 G needle into 10 mL syringes, containing 2 mL of acid citrate dextrose (ACD: 3% (w/v) sodium citrate, 2% (w/v) glucose and 1.5% (w/v) citric acid), each. Platelet rich plasma (PRP) was obtained by centrifugation at 100 *g* for 25 min at room temperature. The PRP was again centrifuged at 800 *g* for 10 min in the presence of 0.1 μg/mL PGI_2 and 0.02 U/mL apyrase. The resulting pellet was resuspended in 2.7 mL of a Ca^{2+}-free modified HEPES buffer (134 mM NaCl, 2.9 mM KCl, 0.34 mM Na_2HPO_4, 12 mM $NaHCO_3$, 1 mM $MgCl_2$, 20 mM HEPES and 5 mM glucose, pH 7.3) and 300 μL ACD with 2.5% (w/v) sodium citrate in the presence of 0.06 μg/mL PGI_2 and 0.015 U/mL apyrase.

2.7. Fluorometric [Ca^{2+}] measurements in platelets

The platelet suspensions were loaded with 4 μM fluo-4/AM for 30 min at room temperature under slow, constant shaking. Platelets were washed by centrifugation (800 x g, 5 min) and resuspended to a concentration of 4–8 × 10^8/mL with Ca^{2+}-free modified HEPES buffer. The FLIPR assay as described above was modified to a four-step addition protocol, comprising the readdition of 1 mM $CaCl_2$, addition of agonists (OAG, GSK1702934 A, C20), inhibition with 1 μM SH045 and stimulation with 0.2 U/mL thrombin.

2.8. Platelet aggregation

Platelet aggregation was studied by monitoring the optical density at 405 nm, using a POLARstar Omega microplate reader (BMG Labtech, Ortenberg, Germany), essentially as described. [25,26] Washed

platelets were adjusted to a density of 2–4 × 10^8 mL^{-1} with modified HEPES buffer, supplemented with 0.1 mg/mL fibrinogen, 2 mg/mL BSA and 1 mM $CaCl_2$, and dispensed into black 96-well plates with clear bottom. The microplate injectors were connected to reservoirs with the respective agonists (thrombin, ADP, OAG, GSK1702934 A), which were added 2 min after starting the measurement, whereas the TRPC6 modulating agents (C20, SH045) were added to each well prior to the measurement. To enable platelet-platelet contact, the microplate was shaken before each cycle (8 s, 700 rpm, double orbital shaking mode). Each measurement consisted of 65 cycles (22 s per cycle) and was performed at 37 °C. The platelet aggregation was determined by normalization to the maximal response induced by 0.2 U/mL thrombin.

2.9. Data presentation and analysis

All data points are presented as means ± SEM. Concentration response curves (fura-2/fluo-4 Ca^{2+} assays and electrophysiology) were generated from at least three independent measurements. In FLIPR experiments, each condition was determined in duplicates. The curves were fitted to a four parameter Hill equation, yielding minimum and maximum effects, half-maximally effective concentrations (EC_{50}) and Hill coefficients for cooperativity. The statistical tests used are given in the respective figure legends. A p-value < 0.05 was considered statistically significant (*).

3. Results

The ChemBioNet compound library includes common pharmacophore moieties and privileged scaffolds that are extracted from the World Drug Index (WDI) and newly arranged to generate a diverse collection of 16,671 drug-like structures [27]. In an attempt to find new activators of the TRPC6 channel, we screened this library on HEK293 cells stably overexpressing hTRPC6-YFP ($HEK_{hTRPC6\text{-}YFP}$) by medium throughput fluorescence imaging plate reader (FLIPR) assays. The cells were loaded with the Ca^{2+} indicator fluo-4 which allows the determination of activating modulators by an increase in the detected fluorescence. In a two-step addition protocol, first the library compounds were injected, before a redundant mix of GPCR stimuli (thrombin, adenosine-5′-triphosphate, carbachol) was applied to the cells as a positive control for the activation of the TRPC6 channel. To circumvent interfering signals by Ca^{2+} mobilization from internal Ca^{2+} stores through GPCR stimulation, 2 μM thapsigargin was used beforehand to deplete intracellular Ca^{2+} stores.

The screening elicited the compound 3-(6,7-dimethoxy-3,3-dimethyl-3,4-dihydroisoquinolin-1-yl)-2*H*-chromen-2-one, termed **C20** (Fig. 1A), which provoked a transient rise of the intracellular Ca^{2+} concentration $[Ca^{2+}]_i$ in $HEK_{hTRPC6\text{-}YFP}$ cells at a concentration of 20 μM (Fig. 1B). The effect can be assigned to a Ca^{2+} influx from the extracellular space via TRPC6, as it did neither appear in Ca^{2+} free measurements nor in native HEK293 cells and was sensitive to the recently published TRPC6 inhibitor SH045 (Fig. 1C). The rise in $[Ca^{2+}]_i$ is concentration-dependent with an apparent EC_{50} value of 2.37 ± 0.25 μM. ınterestingly we found, that **C20** selectively activates TRPC6 and not the closely related ion channels TRPC3 and TRPC7 (Fig. 1D, E; full traces shown in Suppl. Fig. 1). In FLIPR Ca^{2+} measurements, **C20** rather led to a slightly reduced basal activity of the TRPC3 channel and a very weak elevation of the TRPC7 channel activity, which did not reach statistical significance. Thus, **C20** seemed to differ from other known TRPC6 agonists, which do not discriminate between the closely related channels. Prominent examples are OAG (1-oleoyl-1-acetyl-*sn*-glycerol), which is also an activator of PKC, or the recently described activators GSK1702934 A and PPZ1 (Suppl. Fig. 2). The selectivity of **C20** was also proven by further screening of two other representatives of the TRPC group, namely TRPC4 and TRPC5, which were not activated by the compound (Fig. 1F). Exploration of more distantly related TRP family members (TRPM2, TRPM3, TRPM8, TRPV1, TRPV3, TRPV4, TRPA1) revealed a weak (11% of full activation by the specific activator capsaicin) activation of TRPV1 (Fig. 1G and Suppl. Fig.). The compound also strongly activated TRPA1 (up to 134% of activation by 100 μM AITC). A similar effectis observed with many light-absorbing compounds and can presumably be ascribed to a photosensitisation of TRPA1, [28] taking into account, that **C20,** which bears a molecular structure with delocalized π-bonds, absorbs at wavelengths around 400 nm and could lead to the generation of reactive oxygen species (ROS). The fact, that the TRPA1 activation was not reproducible in whole cell patch clamp recordings fits this hypothesis (Suppl. Fig. 3K, L). Apart from a weak reduction of the basal activity of TRPV3, **C20** showed no significant bioactivity on the other tested channels (Fig. 1G).

The scaffold of compound **C20** consists of a coumarin moiety fused to an isoquinoline (Fig. 1A; Table 1). Notably, related structures from the ChemBioNet collection extracted by 2D similarity searches did not evoke rises in $[Ca^{2+}]_i$; even if there were just minor variations in the compound scaffold (see Table 1). To enable more extensive studies and further characterization, we aimed to resynthesize compound **C20**. The synthesis strategy based on previous descriptions of the preparation of 3,3-dialkyl-1-(3-coumarinyl)-3,4-dihydroisoquinolines and was adopted to the reported one-pot-synthesis strategy (Scheme 1)[29,30].

By examining the effect of **C20** on the stimulation of TRPC3, 6 and 7, we observed that **C20** seems to act synergistically with the OAG-induced TRPC6 activation, as the addition the compound further increases the Ca^{2+} response of stimulated cells (Fig. 2A). In the same manner, the presence of low concentrations of **C20** resulted in a remarkable enhancement of the maximal Ca^{2+} response (Fig. 2B), whereas a second addition of OAG or different GPCR agonists in a similar manner would not lead to an enhanced Ca^{2+} signal due to the desensitisation of the channel (Suppl. Fig. 4A, B). Importantly, this **C20**-induced potentiation of TRPC6 activity was not limited to the DAG mimic OAG, as the activation by non-classical activators, like GSK1702934 A, as well as activation by receptor stimulation were also enhanced (Fig. 2C–E). Furthermore, the positive modulation of agonist-induced Ca^{2+} influx in $HEK_{hTRPC6\text{-}YFP}$ by **C20** did not only lead to a significant enhancement of efficacy, but also shifted the EC_{50} of the respective agonist. In FLIPR-based Ca^{2+} measurements, the EC_{50} of OAG on TRPC6 was determined at 40 ± 16 μM and was decreased to 9 ± 0.2 μM in the presence of 10 μM **C20** (see Fig. 2F, G). A similar effect was seen in combination with the non-classical TRPC6 activator GSK1702934 A (Suppl. Fig. 5). These findings suggested an allosteric modulation of the TRPC6 channel by **C20**, which may act as a positive TRPC6 modulator that sensitizes the channel to lower or eventually even basal levels of DAG. To test this hypothesis, we analysed the effect of **C20** in the presence of R59949, which is an inhibitor of type I and II DAG kinases (DAGK), speculating that increased DAG levels would intensify the effect of **C20**. Indeed, incubation of $HEK_{hTRPC6\text{-}YFP}$ with 10 μM R59949 led to significantly higher rises in the Ca^{2+} responses upon stimulation with **C20** alone (Fig. 2 H–J).

In contrast to the strong TRPC6 potentiation, **C20** did not induce a comparable effect on TRPC3 and TRPC7. There, the compound led to a slight inhibition (TRPC3) or to a weak potentiation of TRPC7 at higher concentrations. The agonist-induced stimulation of TRPC4 and TRPC5 was unaffected in the presence of 50 μM **C20** (Fig. 3A–C). The analysis of more distantly related TRP channels showed a slight inhibition of TRPM2 and TRPV2 ($IC_{50} > > 50$ μM) and a weak, but not statistically significant potentiation of TRPV1, TRPV3, TRPV4 and TRPA1 (Fig. 3D).

To test an intervention in the second messenger pathway by activation of phospholipase C (PLC), the translocation of PKCε to the plasma membrane under the influence of **C20** was examined by confocal microscopy. HEK293 cells, stably expressing YFP-tagged PKCε [24] were exposed to **C20** prior to stimulation with phorbol 12-myristate 13-acetate (PMA), which is a highly potent DAG mimic. Exposure of $HEK_{PKC\varepsilon\text{-}YFP}$ cells to **C20** alone did not result in a PKCε-YFP translocation, indicated by an unaltered even distribution of YFP in the cytosol of the cells. In contrast, PMA induced a translocation of the YFP-

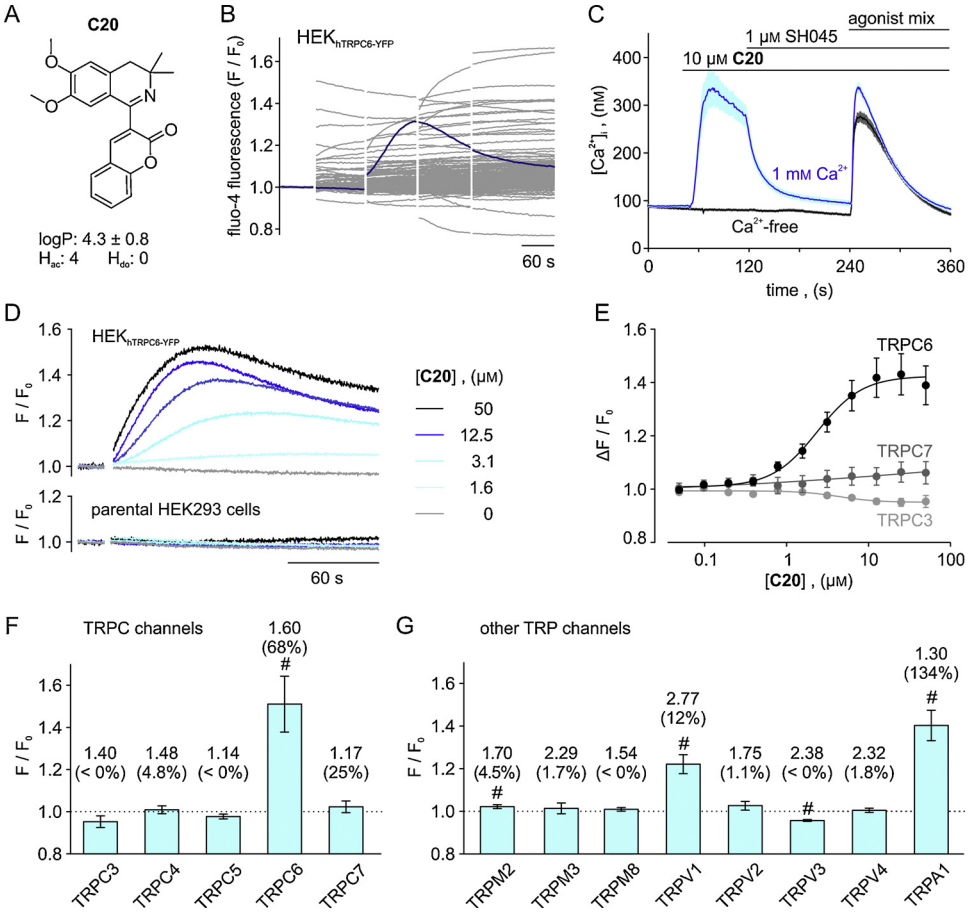

Fig. 1. C20 induces Ca^{2+} influx in HEK cells heterologously expressing TRPC6. (A) Molecular structure of **C20**. (B) Superposition of normalized fluo-4 fluorescence signals (grey lines) from a 384-well plate of the ChemBioNet collection on which compound **C20** was identified as a concentration of 20 µM**C20** provoked a transient Ca^{2+} influx in $HEK_{hTRPC6-YFP}$ cells (blue line). (C) Single cell [Ca^{2+}]$_i$ analysis in fura 2-loaded $HEK_{hTRPC6-YFP}$ cells. TRPC6 activation by **C20** is dependent on extracellular Ca^{2+} and sensitive to the TRPC6 inhibitor **SH045**. (D) **C20** leads to concentration-dependent changes of Fluo-4 fluorescence in $HEK_{hTRPC6-YFP}$ cells but not in parental HEK293 cells. (E) Comparison of concentration-response relationships of **C20** on TRPC3, TRPC6 and TRPC7. (F) Analysis of the effect of 50 µM **C20** on cells stably expressing ion channels of the TRPC family and (G) of more distantly related ion channels. The values above each column indicate the maximal effect of the respective known activators, and the effect of C20 indicated as percentage of maximal effects. Known activators were: 50 µM OAG (TRPC3, TRPC6, TRPC7), 20 nM englerin A (TRPC4, TRPC5), 1 mM H_2O_2 (TRPM2), 50 µM pregnenolone sulfate (TRPM3), 500 µM (-)-menthol (TRPM8), 5 µM capsaicin (TRPV1), 200 µM 2-APB (TRPV2, TRPV3), 200 µM GSK1016790 A (TRPV4), 100 µM AITC (TRPA1). Data were obtained in at least three independent experiments with duplicates, each, and are depicted as means ± S.E.. # $p < 0.05$ compared to baseline by Student's *t* test.

Table 1
Overview of compounds with related structures to C20. The structures were extracted from the ChemBioNet collection by a 2D similarity search using the software ChemFinder 16.0.

compound	R^1	R^2	R^3	TRPC6 potentiation
C20	OMe	OMe		yes
A20	H	H		no
C22	OMe	OMe		no
I22	OMe	OMe		no
I18	OMe	OMe	*n*-butyl	no
K20	OMe	OMe		no

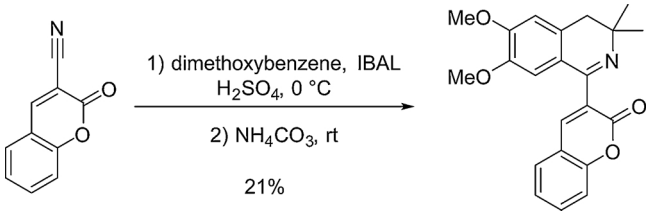

Scheme 1. One-pot-synthesis of 3-(6,7-dimethoxy-3,3-dimethyl-3,4-dihydroisoquinolin-1-yl)-2*H*-chromen-2-one (**C20**).

tagged protein to the plasma membrane (Fig. 4A). In accordance with these results, patch clamp recordings on excised membrane patches of TRPC6-expressing cells point to a direct or membrane-delimited action of **C20** at the TRPC6 channel (Fig. 4B). The application of **C20** to the bath solution resulted in an increased open probability, which was reversible upon washout of the drug. Since TRPC6 typically exhibits very short single channel openings (< 1 ms) [3], these recordings do not allow to conclusively discriminate between a stabilization of the open state and an increased channel availability or an increased single channel conductance.

In line with the results from the initial Ca^{2+} assays, subsequent stimulation with **C20** robustly enhanced OAG-induced currents in whole cell patch clamp studies with TRPC6-expressing cells. This effect was most pronounced for inward currents and became particularly apparent in the current-voltage-relationship, whose shape converged in the presence of **C20** even more to an "n"-like appearance, as shown for activation with 25 µM OAG and subsequent modulation with 5 µM **C20** (Fig. 4D, E). The potentiation was accompanied by an elevated channel noise with increasing positive or negative potentials and could be reversed by washing out the compound. Interestingly, upon modulation with **C20**, the inward currents at negative potentials developed simultaneously with the outward currents at positive potentials, whereas the stimulation with OAG alone showed a delayed development of inward currents (Fig. 4D). When $HEK_{hTRPC6-YFP}$ cells were challenged simultaneously with 10 µM **C20** and 50 µM OAG, the outward current density was increased by the 1.5-fold of the initial value, whereas the physiologically more relevant inward current, attained a six-fold of the maximal OAG-induced current density (Fig. 4F). Similar results were obtained when TRPC6 was stimulated with 300 nM of the non-classical

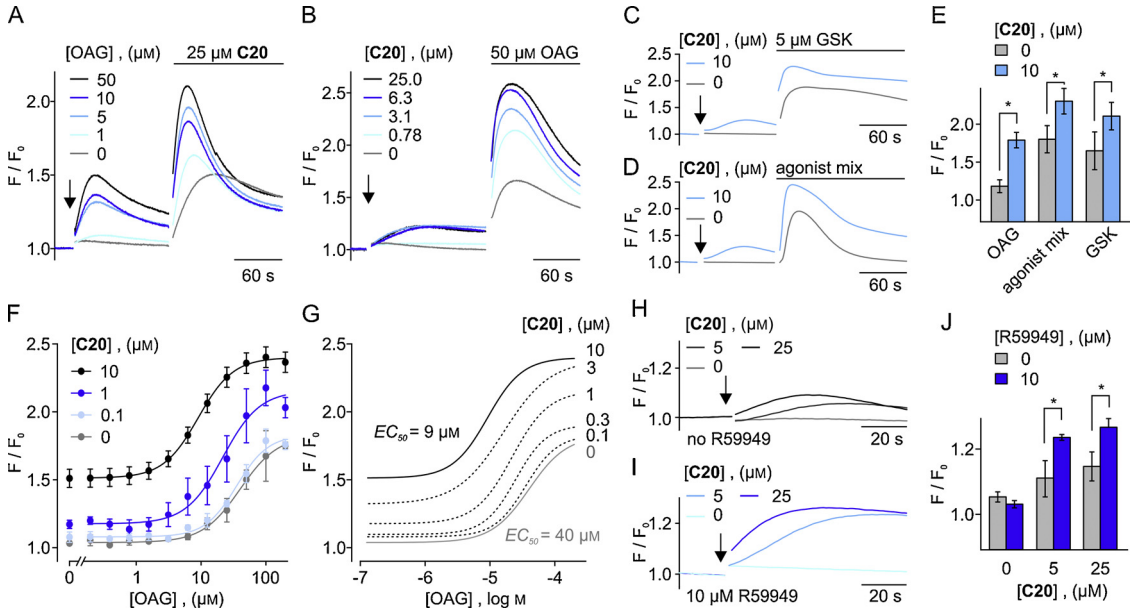

Fig. 2. C20 positively modulates TRPC6. (A–D) Representative FLIPR analyses of TRPC6 stimulation with different activators in combination with **C20**. (A) The Ca^{2+} responses after stimulation with various concentrations of OAG, indicated by fluo 4 fluorescence, are further enhanced by 25 μM **C20**. (B–E) **C20** enhances the maximal activator-induced Ca^{2+} responses in $HEK_{hTRPC6\text{-}YFP}$ cells in a concentration-dependent manner. TRPC6 was stimulated with 50 μM OAG, 5 μM GSK1702934 A, or a redundant mix of GPCR stimuli (1 mM carbachol, 300 μM Na-ATP, 0.5 U/mL thrombin) after incubation with various concentrations of **C20** (* $p < 0.05$, Student's t test). (F, G) Combination of OAG with increasing amounts of **C20** shifts the concentration-response relationship of OAG to lower concentrations. (H–J) Incubation of $HEK_{hTRPC6\text{-}YFP}$ with the DAG kinase inhibitor R59949 (10 μM) prior to treatment with **C20** leads to a significantly enhanced Ca^{2+} response (* $p < 0.01$, Student's *t* test). Data were obtained in at least three independent experiments with duplicates, each, and are depicted as means ± S.E.

activator GSK1702934 A (1.7-fold and 3.8-fold, respectively, Fig. 4F). For evaluating the direct effect on TRPC3 and TRPC7, $HEK_{hTRPC3\text{-}YFP}$ and $HEK_{hTRPC7\text{-}YFP}$ cells were also exposed to OAG and **C20,** and maximal current responses were compared to stimulation with OAG alone. **C20** (10 μM) led to a diminished current response upon TRPC3 stimulation (70% and 55% inhibition of inward and outward currents, respectively), whereas TRPC7 currents were not significantly altered by 10 μM **C20** (Fig. 4F).

To examine the impact of **C20** on native TRPC6-bearing channel complexes, we applied the compound to freshly prepared human platelets, which are reported to express endogenous TRPC6. [7] The treatment with OAG only evoked weak $[Ca^{2+}]_i$ signals in FLIPR measurements, which were strongly and significantly potentiated in the presence of 10 μM **C20**. Again, the potentiation was sensitive to SH045 (Fig. 5A, C). Notably, not only the $[Ca^{2+}]_i$ responses, which result from classical TRPC6 activation (i.e. OAG), were enhanced, but also those induced by the synthetic TPRC3/6/7 activator GSK1702934 A (Fig. 5B, C). Reminiscent to the results in the heterologous cell system, the effect of various concentrations of OAG was also enhanced by subsequent exposure to **C20** (Fig. 5D). Interestingly, **C20** alone did not induce discernible Ca^{2+} signals in platelets, but subsequent treatment with OAG provoked robust rises in $[Ca^{2+}]_i$ (Fig. 5E). The increase in $[Ca^{2+}]_i$ in platelets initiates manifold functional processes, including morphological alterations (shape change) and aggregation [31]. We therefore set out to examine platelet aggregation induced by diverse stimuli, including OAG, in the presence of **C20**. The aggregation was studied in washed platelet suspensions supplemented with 0.1 mg/mL fibrinogen by measuring the decrease in optical density upon stimulation. The stimulation of washed platelets with 0.2 U/mL thrombin led to a rapid aggregation, which was evident by an increase in light transmission. As this response led to maximal aggregation, it served as positive control, to which all other responses were normalized. The platelet aggregation

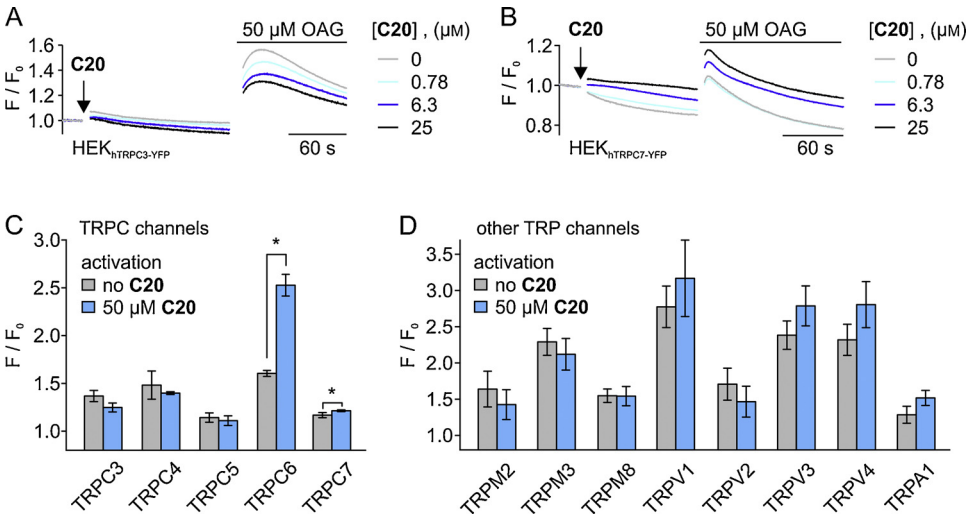

Fig. 3. Analysis of the stimulation of TRP channels in the presence of **C20.** (A) $HEK_{hTRPC3\text{-}YFP}$ and (B) $HEK_{hTRPC7\text{-}YFP}$ cells were challenged with various concentrations of **C20** prior to activation with 50 μM$_{OAG}$. (C)Analysis of the TRPC family of ion channels and (D) of more distantly related ion channels regarding the effect of **C20** on channel activation. Fluo-4-loaded cells were stimulated with respective channel activator: 50 μM OAG (TRPC3, TRPC6, TRPC7), 20 nM englerin A (TRPC4, TRPC5), 1 mM H_2O_2 (TRPM2), 50 μM pregnenolone sulfate (TRPM3), 500 μM (-)-menthol (TRPM8), 5 μM capsaicin (TRPV1), 200 μM 2-APB (TRPV2, TRPV3), 200 μM GSK1016790 A (TRPV4), 100 μM AITC (TRPA1). Data were obtained in at least three independent experiments with duplicates, each, and are depicted as means ± S.E. *$p < 0.05$, Student's *t* test.

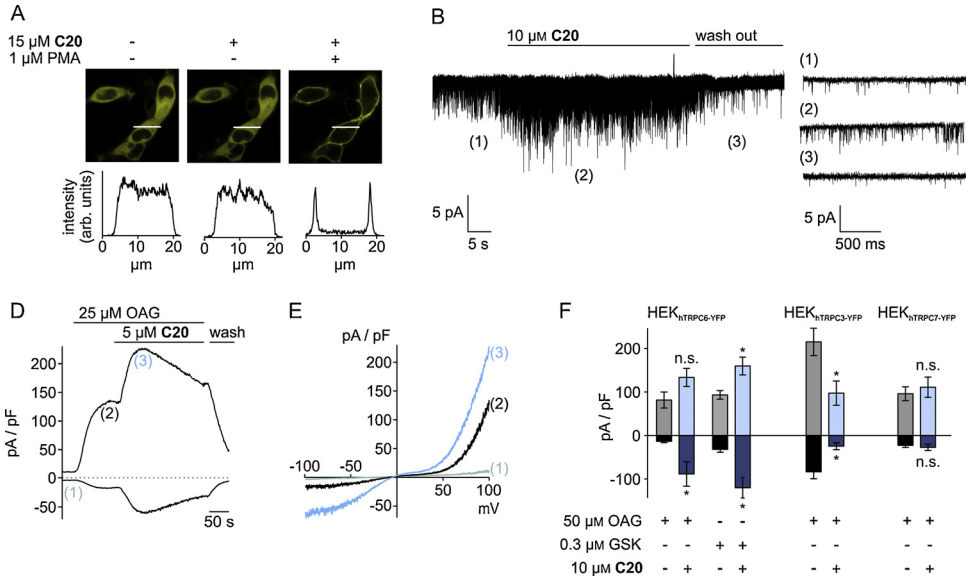

Fig. 4. C20 does not enhance phospholipase C-mediated diacylglycerol formation, but activates TRPC6 currents in isolated membrane patches and in the whole cell mode. (A) Analysis of PKCε-YFP translocation in stably transfected $HEK_{PKCε\text{-}YFP}$ cells by confocal laser scanning microscopy. 10 µM C20, 50 µM OAG and 1 µM PMA were added in intervals of 60 s. The fluorescence intensity profiles (obtained along white line; 22 µM) show the distribution of PKCε-YFP in the cell. (B,C) Representative current traces from inside-out membrane patches excised from $HEK_{hTRPC6\text{-}YFP}$ cells and recorded at −120 mV. $HEK_{hTRPC6\text{-}YFP}$ cells were stimulated with 10 µMc20. (D) Representative whole cell patch-clamp recordings at + 100 mV and − 100 mV and (E) corresponding I–V curves of $HEK_{hTRPC6\text{-}YFP}$ stimulated with 25 µM OAG and 5 µM C20. (F) Comparison of maximal current responses in $HEK_{hTRPC6\text{-}YFP}$ evoked by 50 µM OAG or 0.3 µM GSK1702934 A with or without positive modulation by 10 µM C20. Comparison of maximal current responses in $HEK_{hTRPC3\text{-}YFP}$ and $HEK_{hTRPC7\text{-}YFP}$ cells, evoked by 50 µM OAG, with or without of 10 µM C20. Data represent means ± S.E. (n = 6–9, * $p < 0.05$, Student's *t* test).

was examined by using further agonists, including ADP (10 µM), targeting $P2Y_1$ and $P2Y_{12}$, and collagen (2.5 µg/mL), which induces aggregation by binding to GPVI and GP Ia/IIa [32]. In contrast treatment with thrombin or ADP, collagen-stimulated platelets initially displayed a transiently decreased light transmittance, indicating a shape change response, before aggregation was induced (Fig. 6C). The presence of 10 µMc20had no significant influence on the aggregation induced by these stimuli (Fig. 6D) Conversely, platelet stimulation with OAG (50 or 100 µM) was significantly accelerated and enhanced by addition of 10 µM **C20** (Fig. 6E). The OAG response was insensitive to the known TRPC6 inhibitors SH045 or SAR7334, whereas its potentiation by **C20** was blockable by these inhibitors (shown for SH045 in Fig. 6F). Additionally, when the platelets were treated with 1 µM of the PKC inhibitor bisindolylmaleimide 1 (BIM-1) prior to stimulation, the same amount of OAG failed to induce aggregation (Fig. 6E, lower panel), which is in line with prior studies on TRPC6 in platelets, where it was shown, that platelet aggregation, but not Ca^{2+} entry into platelets (both induced by OAG), is dependent on PKC activity [7]. In line with the fluorometric Ca^{2+} measurements, the increase in aggregation was dependent on the concentration of **C20**. Of note, the positive modulator enabled platelet aggregation at lower OAG concentrations that did not initiate aggregation in the absence of **C20** (Fig. 6G).

4. Discussion

In the present study, we report the discovery of a small molecule TRPC6 modulator, termed **C20**, which was identified by a medium-throughput screening. The compound was found to induce a Ca^{2+} entry through TRPC6 with an apparent EC_{50} value of 2.4 µM. Within the TRPC3/6/7 subfamily, the activation solely occurs on TRPC6, whereas TRPC3 was slightly inhibited in the presence of higher concentrations of the compound and the activity of TRPC7 channels remained almost unaffected. **C20** was also screened towards other members of the TRP family. Importantly, TRPC4 and TRPC5, the closest relatives of TRPC3/6/7 were not modulated by the compound. On more remotely related TRP channels, **C20** mostly showed no significant bioactivity, with the exception of TRPV1 and TRPA1, whose slight activation by **C20** at higher concentrations might be explained by a photosensitizing effect and the generation of ROS during irradiation with blue or ultraviolet light [28,33]. Whether **C20** also acts on other channel entities, like

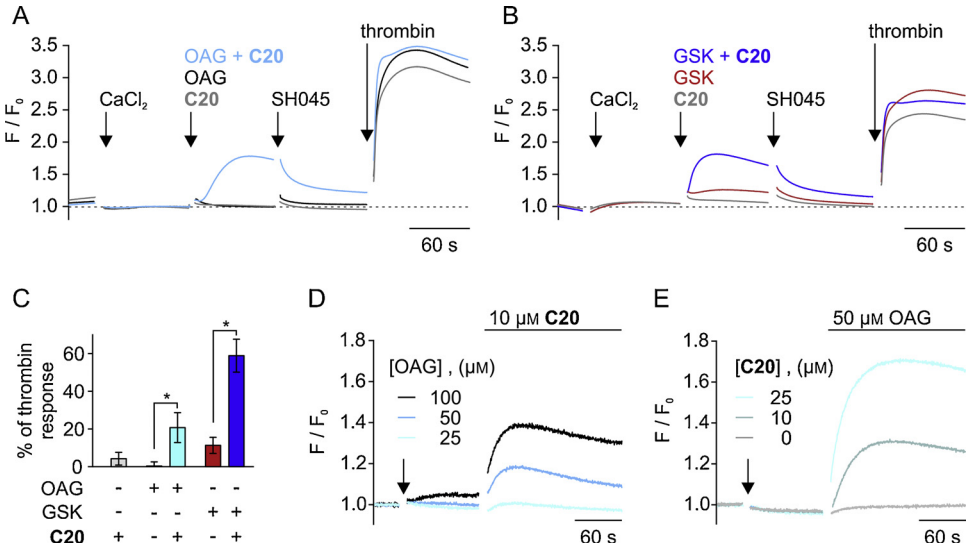

Fig. 5. C20 induces Ca^{2+} influx in human platelets. (A) FLIPR Ca^{2+} measurements in washed human platelets. After recalcification (1 mM $CaCl_2$), platelets were exposed to 50 µM OAG and 10 µM C20, alone or in combination prior to addition of 1 µM of the TRPC6 channel blocker SH045. In a last step, platelets were activated by treatment with 0.2 U/mL thrombin. (B) Same experiment as in (A), but with 5 µM GSK1702934 A instead of OAG. (C) Ca^{2+} responses of platelets induced by diverse stimuli (50 µM OAG, 5 µM GSK1702944 A, 10 µM C20), normalized to the thrombin signal. Data were obtained from 7 individuals with quadruplets, each. Shown are means ± SD (* $p < 0.05$, Student's t test). (D) Washed platelets were stimulated with various concentrations of OAG prior to treatment with 10 µM **C20**. (E) Washed platelets were stimulated with various concentrations of **C20** prior to treatment with 50 µM OAG.

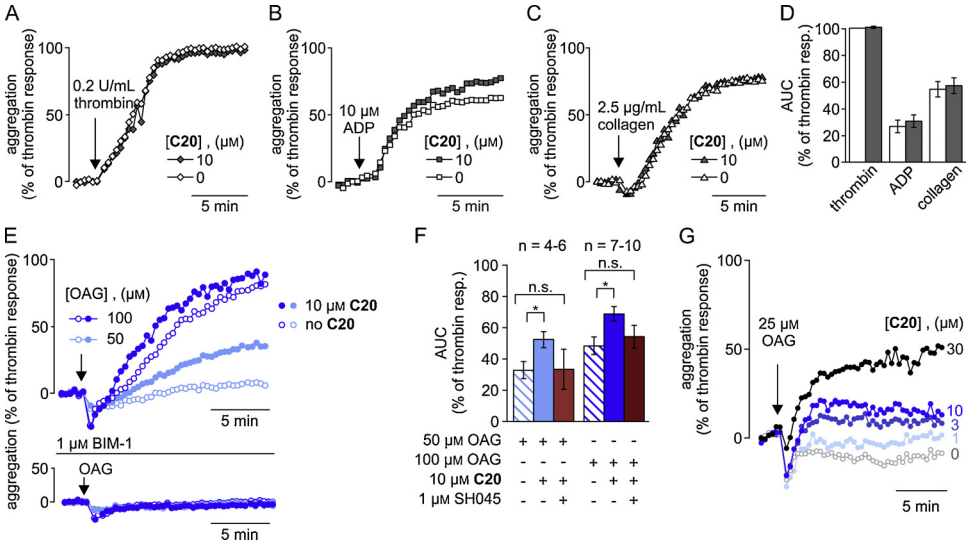

Fig. 6. Effect of **C20** on platelet aggregation in response to diverse stimuli. Representative aggregation measurements with washed platelets, recorded on a plate reader by monitoring changes in optical density. The stimulation with 0.2 U/mL thrombin served as a positive control, to which responses were normalized. (A–C) Platelets were challenged with various aggregation-inducing agonists (0.2 U/mL thrombin, 10 µM ADP, 2.5 µg/mL collagen) with or without 10 µM**C20**.(D)Statistical analysis of several experiments by comparison of the area under the curve (AUC, normalized to thrombin response without **C20**). Data represent means ± S.E. (n = 4–10). (E) Platelets were challenged with 50 µM or 100 µM OAG with or without 10 µM C20 (upper panel) and in the presence of the protein kinase C inhibitor BIM-1 (1 µM) preincubated for 5 min prior to the start of the recording (lower panel). (F) Statistical analysis of several experiments by comparison of AUC (normalized to thrombin response). Data represent means ± S.E. (n = 4–10, two-sample *t* test, *p < 0.05). (G) Platelets were challenged with various concentrations of **C20** (0–30 µM) prior to treatment with 25 µM OAG.

voltage-gated Ca^{2+} or Na^{+} channels, or on G-protein coupled receptors was not tested so far and requires further investigation. However, we demonstrated that **C20** does not interfere with PLC signalling. In further studies we observed a significant enhancement of agonist-induced TRPC6 activation when **C20** was simultaneously applied. Moreover, the presence of **C20** did not only enhance the maximal effects of activation, but also shifted the concentration-response relationship of OAG to lower concentrations. Hence, the compound can be regarded as a positive allosteric modulator (PAM) of TRPC6 channels. Although we could not elucidate the exact mechanism of action, we can speculate, that binding of **C20** to TRPC6 sensitizes the channel to lower concentrations of diacylglycerols. This might explain the fact, that **C20** alone also leads to a rise in $[Ca^{2+}]_i$ in cells heterologously expressing TRPC6. The finding that an inhibition of DAG kinases leads to an enhanced Ca^{2+} influx upon stimulation with **C20**, fits this hypothesis.

At presence, no reliable activators are known that selectively act on TRPC6, even though there are some candidates, which are widely used for this purpose. The natural products hyperforin from St. John's wort, which has been used for centuries for the treatment of depressive disorders, has been described in 2007 as a selective activator of TRPC6. The bioactivity is supposed to base on similar pharmacophoric properties of OAG and hyperforin, whereat the selectivity towards TRPC3 and TRPC7 is explained through the rigid scaffold of hyperforin compared to OAG [34,35]. However, the TRPC6-specific action is controversial, as hyperforin-induced currents do not display the typical current/voltage characteristics and are also found in not-TRPC6 expressing cell types, which was recently ascribed to a TRPC-independent, protonophoric action of this compound [36]. The cyclooxygenase inhibitor flufenamic acid, which was already developed in the 60′s, was also commonly used as unspecific inhibitor of cation channels [37,38]. It was found, that the compound had a potentiating effect on TRPC6, but not on TRPC3 and TRPC7, and the use of flufenamate enabled the detection of native TRPC6 currents in smooth muscle cells of the portal vein from rats and pulmonary epithelium [39,40]. However, due to its off-target effects and the recently described flufenamate-induced inhibition of TRPC6, also the application of flufenamic acid as a TRPC6-selective activator is not unquestionable [41].

Of note, less is known about positive allosteric modulation of TRP channels mediated by small molecules, although some examples can be found in the regulation of thermoregulated TRPs. A 1.4dihydropyridine derivative (MRS1477) has been reported to positively modulate the TRPV1 channel. The channel has already been described before to be allosterically modulated, as the activation by protons or vanilloid ligands is taking place at structurally different sites at the channel [42,43]. For MRS1477, an interaction with the pore forming loop between the transmembrane regions 5 and 6 has been hypothesized, which directly and independently of the applied activator affects channel gating, without having an intrinsic agonist or antagonist activity [44]. Just recently, another example for a small molecule positive TRP-modulator has been reported. Synthetic inhibitors of COX-2 (coxibs) proved to positively modulate TRPV3-activity upon 2-APB stimulation as well as thermoactivation [45]. With **C20** we firstly describe a similar mechanism apart from TRPV channels, although the underlying mechanism of **C20**-induced TRPC6 potentiation will have to be further explored. The results from inside-out single channel measurements seem to indicate, that **C20** acts in a membrane-delimited fashion without the need of other intracellular components. Despite the fact that these recordings did not reveal the exact mode of action of C20 at the single channel level, the preferential potentiation of inward currents that was associated with an increased current noise (e.g. in Fig. 4E) point to a preferential increase in channel availability at negative membrane potentials. The binding site for C20 is currently unknown. Based on cryo-electron microscopy imaging studies, a structural model of TRPC6 is available, including the site of an inhibitory modulator [46]. Whether C20 occupies the same or an overlapping binding site, remains to be investigated.

The expression of TRPC6 in murine and human platelets is well described [7] and there is evidence, that the channel takes part in receptor-operated calcium entry (ROCE), as studies with murine TRPC6$^{-/-}$ platelets revealed a decreased Ca^{2+} influx upon stimulation by OAG. The exact role of TRPC6 regulating the platelet function remains, however, ambiguous. Further reports from experiments with TRPC6-deficient mice provided rather disputable results. Some studies reported a lack of phenotype in TRPC6-deficient mice regarding platelet responses and haemostasis and, therefore, suggested a minor physiological and pathophysiological role of TRPC6 in platelets [47–50]. Contradicting these reports, other studies describe a prolonged tail bleeding time and a delayed thrombus formation in TRPC6$^{-/-}$ mice [51]. In studies on human platelets we found, that **C20** leads to a significantly enhanced Ca^{2+} influx when combined with TRPC6-activating compounds like OAG or GSK1792934 A. Importantly, we also observed a significantly increased platelet aggregation when **C20**-treated platelets were stimulated with OAG, but not when stimulated with other aggregation-inducing agonists like ADP or collagen. Since the application

of the recently published TRPC6 inhibitor SH045 counteracted the positive effect of C20 on OAG-induced aggregation, we conclude that the effect indeed involves TRPC6. On the other hand, the TRPC6 inhibitor did not influence the OAG- or thrombin-induced aggregation in the absence of C20. Therefore, we agree with previously made observations that TRPC6 seems not to be a critical component in platelet aggregation induced by commonly used hormonal or physiological stimuli. Its role in platelet Ca^{2+} homeostasis may, therefore, contribute to more subtle changes in agonist sensitivity or to other platelet responses.

The ability to selectively amplify TRPC6 responses in heterologous cell systems as well as in native tissues makes **C20** a valuable pharmacological tool. We, therefore, refer to C20 as TRPC6-PAM-C20. Furthermore, TRPC6-PAM-C20 fulfils the criteria of drug likeness (Lipinski's rule of five) and is easily prepared in a one-step and one-pot synthesis and, therefore, readily available for biological studies. Particularly with regard to studies in native systems, the sensitizing ability of a positive allosteric modulator like TRPC6-PAM-C20 can assist to elucidate still unidentified roles of TRPC6 in other tissues or organs.

Funding

This work was supported by the Deutsche Forschungsgemeinschaft DFG, SFB TRR 152, Project P18.

Acknowledgements

We thank Johannes Broichhagen, Max-Planck-Institute for Medical Research, Heidelberg, Germany, for the analytical support in characterizing chemical properties of the TRPC6-PAM C20.

Appendix A. Supplementary data

Supplementary material related to this article can be found, in the online version, at doi:https://doi.org/10.1016/j.ceca.2018.12.009.

References

[1] R.C. Hardie, B. Minke, The trp gene is essential for a light-activated Ca2+ channel in Drosophila photoreceptors, Neuron 8 (1992) 643–651.
[2] D.E. Clapham, D. Julius, C. Montell, G. Schultz, International Union of Pharmacology. XLIX. Nomenclature and structure-function relationships of transient receptor potential channels, Pharmacol. Rev. 57 (2005) 427–450.
[3] T. Hofmann, A.G. Obukhov, M. Schaefer, C. Harteneck, T. Gudermann, G. Schultz, Direct activation of human TRPC6 and TRPC3 channels by diacylglycerol, Nature 397 (1999) 259–263.
[4] R. Inoue, T. Okada, H. Onoue, Y. Hara, S. Shimizu, S. Naitoh, Y. Ito, Y. Mori, The transient receptor potential protein homologue TRP6 is the essential component of vascular alpha(1)-adrenoceptor-activated Ca(2+)-permeable cation channel, Circ. Res. 88 (2001) 325–332.
[5] G.A. Nagy, G. Botond, Z. Borhegyi, N.W. Plummer, T.F. Freund, N. Hájos, DAG-sensitive and Ca(2+) permeable TRPC6 channels are expressed in dentate granule cells and interneurons in the hippocampal formation, Hippocampus 23 (2013) 221–232.
[6] J. Reiser, K.R. Polu, C.C. Möller, P. Kenlan, M.M. Altintas, C. Wei, C. Faul, S. Herbert, I. Villegas, C. Avila-Casado, M. McGee, H. Sugimoto, D. Brown, R. Kalluri, P. Mundel, P.L. Smith, D.E. Clapham, M.R. Pollak, TRPC6 is a glomerular slit diaphragm-associated channel required for normal renal function, Nat. Genet. 37 (2005) 739–744.
[7] S.R. Hassock, M.X. Zhu, C. Trost, V. Flockerzi, K.S. Authi, Expression and role of TRPC proteins in human platelets: evidence that TRPC6 forms the store-independent calcium entry channel, Blood 100 (2002) 2801–2811.
[8] K.S. Authi, TRP channels in platelet function, Handb. Exp. Pharmacol. (2007) 425–443.
[9] Y. Yu, S.H. Keller, C.V. Remillard, O. Safrina, A. Nicholson, S.L. Zhang, W. Jiang, N. Vangala, J.W. Landsberg, J.-Y. Wang, P.A. Thistlethwaite, R.N. Channick, I.M. Robbins, J.E. Loyd, H.A. Ghofrani, F. Grimminger, R.T. Schermuly, M.D. Cahalan, L.J. Rubin, J.X.-J. Yuan, A functional single-nucleotide polymorphism in the TRPC6 gene promoter associated with idiopathic pulmonary arterial hypertension, Circulation 119 (2009) 2313–2322.
[10] M.P. Winn, A mutation in the TRPC6 cation channel causes familial focal segmental glomerulosclerosis, Science 308 (2005) 1801–1804.
[11] M. Riehle, A.K. Büscher, B.-O. Gohlke, M. Kaßmann, M. Kolatsi-Joannou, J.H. Bräsen, M. Nagel, J.U. Becker, P. Winyard, P.F. Hoyer, R. Preissner, D. Krautwurst, M. Gollasch, S. Weber, C. Harteneck, TRPC6 G757D loss-of-function mutation associates with FSGS, J. Am. Soc. Nephrol. 27 (2016) 2771–2783.
[12] C. Harteneck, C. Klose, D. Krautwurst, Synthetic modulators of TRP channel activity, Adv. Exp. Med. Biol. 704 (2011) 87–106.
[13] N. Urban, K. Hill, L. Wang, W.M. Kuebler, M. Schaefer, Novel pharmacological TRPC inhibitors block hypoxia-induced vasoconstriction, Cell Calcium 51 (2012) 194–206.
[14] T. Maier, M. Follmann, G. Hessler, H.-W. Kleemann, S. Hachtel, B. Fuchs, N. Weissmann, W. Linz, T. Schmidt, M. Lohn, K. Schroeter, L. Wang, H. Rutten, C. Strübing, Discovery and pharmacological characterization of a novel potent inhibitor of diacylglycerol-sensitive TRPC cation channels, Brit. J. Pharmacol. 172 (2015) 3650–3660.
[15] S. Häfner, F. Burg, M. Kannler, N. Urban, P. Mayer, A. Dietrich, D. Trauner, J. Broichhagen, M. Schaefer, A (+)-larixol congener with high affinity and subtype selectivity toward TRPC6, ChemMedChem 13 (2018) 1028–1035.
[16] X. Xu, I. Lozinskaya, M. Costell, Z. Lin, J.A. Ball, R. Bernard, D.J. Behm, J.P. Marino, C.G. Schnackenberg, Characterization of small molecule TRPC3 and TRPC6 agonist and antagonists, Biophys. J. 104 (2013) 454.
[17] S. Sawamura, M. Hatano, Y. Takada, K. Hino, T. Kawamura, J. Tanikawa, H. Nakagawa, H. Hase, A. Nakao, M. Hirano, R. Rotrattanadumrong, S. Kiyonaka, M.X. Mori, M. Nishida, Y. Hu, R. Inoue, R. Nagata, Y. Mori, Screening of transient receptor potential canonical channel activators identifies novel neurotrophic piperazine compounds, Mol. Pharmacol. 89 (2016) 348–363.
[18] C. Qu, M. Ding, Y. Zhu, Y. Lu, J. Du, M. Miller, J. Tian, J. Zhu, J. Xu, M. Wen, A. Er-Bu, J. Wang, Y. Xiao, M. Wu, O.B. McManus, M. Li, J. Wu, H.-R. Luo, Z. Cao, B. Shen, H. Wang, M.X. Zhu, X. Hong, Pyrazolopyrimidines as potent stimulators for transient receptor potential canonical 3/6/7 channels, J. Med. Chem. 60 (2017) 4680–4692.
[19] N. Urban, L. Wang, S. Kwiek, J. Rademann, W.M. Kuebler, M. Schaefer, Identification and validation of larixyl acetate as a potent TRPC6 inhibitor, Mol. Pharmacol. 89 (2016) 197–213.
[20] H. Beckmann, J. Richter, K. Hill, N. Urban, H. Lemoine, M. Schaefer, A benzothiadiazine derivative and methylprednisolone are novel and selective activators of transient receptor potential canonical 5 (TRPC5) channels, Cell Calcium 66 (2017) 10–18.
[21] J.C. Lenz, H.P. Reusch, N. Albrecht, G. Schultz, M. Schaefer, Ca2+-controlled competitive diacylglycerol binding of protein kinase C isoenzymes in living cells, J. Cell Biol. 159 (2002) 291–302.
[22] A. Edelstein, N. Amodaj, K. Hoover, R.D. Vale, N. Stuurman, Computer control of microscopes using μManager, Curr. Protoc. Mol. Biol. (2010) 20 Chapter 14.
[23] M.D. Abràmoff, P.J. Magalhães, S.J. Ram, Image processing with ImageJ, Biophotonics Int. 11 (2004) 36–42.
[24] M. Schaefer, N. Albrecht, T. Hofmann, T. Gudermann, G. Schultz, Diffusion-limited translocation mechanism of protein kinase C isotypes, FASEB J. 15 (2001) 1634–1636.
[25] B. Bednar, C. Condra, R.J. Gould, T.M. Connolly, Platelet aggregation monitored in a 96 well microplate reader is useful for evaluation of platelet agonists and antagonists, Thromb. Res. 77 (1995) 453–463.
[26] S. Vaiyapuri, J.M. Gibbins, Miniaturised platelet aggregation assays using the NOVOstar microplate reader, BMG Labtech Rev. 04 (2011).
[27] M. Lisurek, B. Rupp, J. Wichard, M. Neuenschwander, J.P. von Kries, R. Frank, J. Rademann, R. Kühne, Design of chemical libraries with potentially bioactive molecules applying a maximum common substructure concept, Mol. Divers. 14 (2010) 401–408.
[28] K. Hill, M. Schaefer, Ultraviolet light and photosensitising agents activate TRPA1 via generation of oxidative stress, Cell Calcium 45 (2009) 155–164.
[29] A.G. Mikhailovskii, M.I. Vahrin, Synthesis of 3,3-Dialkyl-1-(3-coumarinyl)-3,4-dihydroisoquinolines, Chem. Heterocyc. Compd. 40 (2004) 1036–1038.
[30] Y.V. Shklyaev, M.A. Yeltsov, Y.S. Rozhkova, A.G. Tolstikov, V.M. Dembitsky, A new approach to synthesis of 3,3-dialkyl-3,4-dihydroisoquinoline derivatives, Heteroatom Chem. 15 (2004) 486–493.
[31] D. Varga-Szabo, A. Braun, B. Nieswandt, Calcium signaling in platelets, J. Thromb. Haemost. 7 (2009) 1057–1066.
[32] M. Moroi, S.M. Jung, Platelet receptors for collagen, Thromb. Haemost. 78 (1997) 439–444.
[33] A. Babes, S.K. Sauer, L. Moparthi, T.I. Kichko, C. Neacsu, B. Namer, M. Filipovic, P.M. Zygmunt, P.W. Reeh, M.J.M. Fischer, Photosensitization in porphyrias and photodynamic therapy involves TRPA1 and TRPV1, J. Neurosci. 36 (2016) 5264–5278.
[34] K. Leuner, V. Kazanski, M. Müller, K. Essin, B. Henke, M. Gollasch, C. Harteneck, W.E. Müller, Hyperforin–a key constituent of St. John's wort specifically activates TRPC6 channels, FASEB J. 21 (2007) 4101–4111.
[35] K. Leuner, J.H. Heiser, S. Derksen, M.I. Mladenov, C.J. Fehske, R. Schubert, M. Gollasch, G. Schneider, C. Harteneck, S.S. Chatterjee, W.E. Müller, Simple 2,4-diacylphloroglucinols as classic transient receptor potential-6 activators–identification of a novel pharmacophore, Mol. Pharmacol. 77 (2010) 368–377.
[36] T.S. Sell, T. Belkacemi, V. Flockerzi, A. Beck, Protonophore properties of hyperforin are essential for its pharmacological activity, Sci. Rep. 4 (2014) 7500.
[37] C.V. Winder, J. Wax, B. Serrano, E.M. Jones, M.L. McPhee, Anti-inflammatory and antipyretic properties of N-(alpha,alpha,alpha-trifluoro-m-tolyl) anthranilic acid (CI-440; flufenamic acid), Arthritis Rheum. 6 (1963) 36–47.
[38] R. Guinamard, C. Simard, C. Del Negro, Flufenamic acid as an ion channel modulator, Pharmacol. Therapeut. 138 (2013) 272–284.
[39] K. Yamada, Y. Waniishi, R. Inoue, Y. Ito, Fenamates potentiate the alpha 1-adrenoceptor-activated nonselective cation channels in rabbit portal vein smooth muscle, Jpn. J. Pharmacol. 70 (1996) 81–84.

[40] N. Weissmann, A. Sydykov, H. Kalwa, U. Storch, B. Fuchs, M. Mederos y Schnitzler, R.P. Brandes, F. Grimminger, M. Meissner, M. Freichel, S. Offermanns, F. Veit, O. Pak, K.-H. Krause, R.T. Schermuly, A.C. Brewer, Harald H.H.W. Schmidt, W. Seeger, A.M. Shah, T. Gudermann, H.A. Ghofrani, A. Dietrich, Activation of TRPC6 channels is essential for lung ischaemia-reperfusion induced oedema in mice, Nat. Commun. 3 (2012) 649.
[41] C. Klose, I. Straub, M. Riehle, F. Ranta, D. Krautwurst, S. Ullrich, W. Meyerhof, C. Harteneck, Fenamates as TRP channel blockers: mefenamic acid selectively blocks TRPM3, Brit. J. Pharmacol. 162 (2011) 1757–1769.
[42] N.R. Gavva, R. Tamir, L. Klionsky, M.H. Norman, J.-C. Louis, K.D. Wild, J.J.S. Treanor, Proton activation does not alter antagonist interaction with the capsaicin-binding pocket of TRPV1, Mol. Pharmacol. 68 (2005) 1524–1533.
[43] S. Ryu, B. Liu, J. Yao, Q. Fu, F. Qin, Uncoupling proton activation of vanilloid receptor TRPV1, J. Neurosci. 27 (2007) 12797–12807.
[44] K. Kaszas, J.M. Keller, C. Coddou, S.K. Mishra, M.A. Hoon, S. Stojilkovic, K.A. Jacobson, M.J. Iadarola, Small molecule positive allosteric modulation of TRPV1 activation by vanilloids and acidic pH, J. Pharmacol. Exp. Ther. 340 (2012) 152–160.
[45] S. Spyra, A. Meisner, M. Schaefer, K. Hill, COX-2-selective inhibitors celecoxib and deracoxib modulate transient receptor potential vanilloid 3 channels, Brit. J. Pharmacol. 174 (2017) 2696–2705.
[46] Q. Tang, W. Guo, L. Zheng, J.-X. Wu, M. Liu, X. Zhou, X. Zhang, L. Chen, Structure of the receptor-activated human TRPC6 and TRPC3 ion channels, Cell Res. (2018).
[47] L. Albarran, A. Berna-Erro, N. Dionisio, P.C. Redondo, E. Lopez, J.J. Lopez, G.M. Salido, J.M. Brull Sabate, J.A. Rosado, TRPC6 participates in the regulation of cytosolic basal calcium concentration in murine resting platelets, Biochim. Biophys. Acta 1843 (2014) 789–796.
[48] G. Ramanathan, S. Gupta, I. Thielmann, I. Pleines, D. Varga-Szabo, F. May, C. Mannhalter, A. Dietrich, B. Nieswandt, A. Braun, Defective diacylglycerol-induced Ca2+ entry but normal agonist-induced activation responses in TRPC6-deficient mouse platelets, J. Thromb. Haemost. 10 (2012) 419–429.
[49] A. Berna-Erro, L. Albarran, N. Dionisio, P.C. Redondo, N. Alonso, L.J. Gomez, G.M. Salido, J.A. Rosado, The canonical transient receptor potential 6 (TRPC6) channel is sensitive to extracellular pH in mouse platelets, Blood Cells Mol. Dis. 52 (2014) 108–115.
[50] H.P. Vemana, Z.A. Karim, C. Conlon, F.T. Khasawneh, A critical role for the transient receptor potential channel type 6 in human platelet activation, PLoS One 10 (2015) e0125764.
[51] E.V. Paez Espinosa, J.P. Murad, H.J. Ting, F.T. Khasawneh, Mouse transient receptor potential channel 6: Role in hemostasis and thrombogenesis, Biochem. Bioph. Res. Commun. 417 (2012) 853–856.